Applied Clay Science 212 (2021) 106233

Contents lists available at ScienceDirect

Applied Clay Science

journal homepage: www.elsevier.com/locate/clay

Research Paper

Conventional or mechanochemically-aided intercalation of diclofenac and naproxen anions into the interlamellar space of CaFe-layered double hydroxides and their application as dermal drug delivery systems☆

Márton Szabados [a,b], Attila Gácsi [b,c], Yvette Gulyás [b], Zoltán Kónya [d,e], Ákos Kukovecz [d], Erzsébet Csányi [c], István Pálinkó [a,b], Pál Sipos [b,f,*]

[a] Department of Organic Chemistry, University of Szeged, Dóm tér 8, Szeged H-6720, Hungary
[b] Material and Solution Structure Research Group, Institute of Chemistry, University of Szeged, Aradi vértanúk tere 1, Szeged H-6720, Hungary
[c] Institute of Pharmaceutical Technology and Regulatory Affairs, University of Szeged, Eötvös utca 6, Szeged H-6720, Hungary
[d] Department of Applied and Environmental Chemistry, University of Szeged, Rerrich B. tér 1, Szeged H-6720, Hungary
[e] MTA-SZTE Reaction Kinetics and Surface Chemistry Research Group, Rerrich B. tér 1, Szeged H-6720, Hungary
[f] Department of Inorganic and Analytical Chemistry, University of Szeged, Dóm tér 7, Szeged H-6720, Hungary

ARTICLE INFO

Keywords:
Layered double hydroxides (LDH)
CaFe-LDH
Intercalation
Diclofenac
Naproxen
Anti-inflammatory drugs
Controlled release
Structural and surface characterization
In vitro and *ex vivo* release tests

ABSTRACT

The intercalation/encapsulation of the anionic forms of diclofenac and naproxen anti-inflammatory drugs into CaFe-layered double hydroxides (LDHs) were investigated by four techniques. A novel mechanochemically-aided pathway was used and compared to the conventional co-precipitation, direct anion exchange and dehydroxylation-rehydration routes. The evolved average crystal thicknesses (23–35 nm) showed good correlation with the high drug-loading content (26–55% w/w) of the LDH solids. The as-prepared hybrid nanocomposites were studied in detail by X-ray diffractometry, Fourier-transform infrared and Raman spectroscopies, scanning electron microscopy, thermogravimetric and dynamic light scattering analyses. The drug–LDH solids were dispersed in hydrogels and the light microscopic size analysis imaged particles mainly of area between 5 and 10 μm^2. In Franz diffusion cells, the *in vitro* drug release tests (collated by the Korsmeyer–Peppas kinetic model) registered slow release of the organic molecules from the external surface and the interlayer region of the LDH particles highly depending on the applied intercalation techniques. Compared to hydrogels without LDH solids, the liberation of drug molecules were found to be 15–70% slower from their LDH-capsulated forms. Raman mapping of the *ex vivo* human skin penetration tests visualized the transdermal route of the drug molecules and attested their accumulation in the epidermis and upper zone of the dermis from the LDH − hydrogel preparations.

1. Introduction

Layered double hydroxide (LDH) materials have the frequently occurring CdI_2 structure in their natural mineral form (the first member was discovered in Snarum, Norway as the accompanying deposit of soapstone (Hochstetter, 1842)), but for application they are synthesized, mostly without difficulties (Evans and Slade, 2006; Duan et al., 2011). They are anionic clay-type materials and their framework are derived from brucite-like ($Mg(OH)_2$) layered $M(OH)_2$ solids (where commonly M = Mg^{2+}, Ca^{2+}, Mn^{2+}, Ni^{2+}, Co^{2+}, Cu^{2+}or Zn^{2+}) *via* isomorphous substitution of divalent cations by trivalent (Al^{3+}, V^{3+}, Cr^{3+}, Fe^{3+}, Ga^{3+}). The incorporation of the guest metal cations of higher valence results in positively charged layers, therefore, hydrated organic/inorganic anions have to be, and indeed they are intercalated/encapsulated among the layers as charge compensators. The stoichiometry of most LDH variants can be described with the following formula: $[M(II)_{1-x}M(III)_x(OH)_2]^{x+}[A^{m-}_{x/m}\cdot nH_2O)]^{x-}$, where *M* stands for the di- and trivalent metal ions, $x = M(III)/[M(II) + M(III)]$ and A^{m-} designates the *m*-

☆ This publication is dedicated to the memory of our mentor, friend and colleague, Prof. István Pálinkó, who passed away shortly after the submission of the current manuscript.

* Corresponding author at: Material and Solution Structure Research Group, Institute of Chemistry, University of Szeged, Aradi vértanúk tere 1, Szeged H-6720, Hungary.
E-mail address: sipos@chem.u-szeged.hu (P. Sipos).

https://doi.org/10.1016/j.clay.2021.106233
Received 15 January 2021; Received in revised form 5 July 2021; Accepted 27 July 2021
Available online 31 July 2021

charged exchangeable interlayer anions (Miyata, 1983; Forano et al., 2006). Owing to their simply and widely tunable compositions, they have received exceptional attention in the last decades as catalyst or catalyst support primarily (Fan et al., 2014; Sipos and Pálinkó, 2018), but their potential application areas include a wide area starting from the polymer industry (fire retardant and biodegradable additives, Ray and Okamoto, 2003), through water (He et al., 2018; Somosi et al., 2019) and gas treatment (adsorbers and anion exchangers, Ding and Alpay, 2001; Kameda et al., 2020) to medical supply as novel antacids or containers of medicine molecules in anionic forms (Del Hoyo, 2007) or even fluoride source in dentistry (Hoxha et al., 2019).

The representatives of hydrocalumites form a subgroup of LDH materials, where the M(II) cations are exclusively calcium ions (Taylor, 1973; Mills et al., 2012). The incorporation of the tri- and tetravalent metal cations into the structure of the portlandite ($Ca(OH)_2$) always occur with the fixed $x = 0.33$ value, due to the relatively large-sized calcium ions, and hence, the heptacoordination (instead of the common octahedral coordination of other $M(OH)_2$) spheres around the Ca (II) (Rousselot et al., 2002). The seventh apex of Ca-polyhedron means an extra coordination site occupied by water molecules or interlayer anions, thus these solids have enhanced anion-exchange capabilities (Renaudin et al., 1999; Chen et al., 2015). In recent years, their wide-ranging and technologically promising utilizations were successfully demonstrated from the area of water treatment (Zhang and Reardon, 2005), to catalytic synthesises (Sipos and Pálinkó, 2018; Kuwahara et al., 2012) *via* healthcare (Kim and Oh, 2016; Linares et al., 2016; Fontes et al., 2016; Saha et al., 2017), polymer (Vieille et al., 2003) and even electrochemistry (Soussou et al., 2017).

The large variety of trivalent cations in the layers and the charge-compensating anions among the layers attracted the development of numerous synthesis and intercalation techniques. In general, the hydrocalumites are prepared by the co-precipitation method; in this technique the evolution of the layered structure and the introduction of the appropriate interlamellar anions take place in parallel (Rousselot et al., 2002; Dékány and Haraszti, 1997; Szabados et al., 2019a). The so-called urea, sol-gel hydrolysis (Mora et al., 2011) and hydrothermal methods (Renaudin et al., 1999) are similarly well-explored techniques, but several mechanochemically aided and pure mechanochemical (Szabados et al., 2018; Qu et al., 2019a) syntheses are also applied for the preparation of hydrocalumites with exotic metal ions like Sn^{4+} or Ti^{4+} (Ferencz et al., 2014; Qu et al., 2019b) in the layers, especially when the conventional methods fail. During these types of syntheses, one has to take into account the limitation of the anion exchange capability of the LDH solids related to the intercalation tendency of the anions. The strength of electrostatic interaction between the interlamellar anions and the host sheets are well specified by the lyotropic series of the anions in which the large organic molecules with low charge densities are generally placed behind the simple inorganic anions (Miyata, 1983; Forano et al., 2006).

As alternative routes to encapsulate larger anions into the hydrocalumites, the dehydroxylation-rehydration and the delamination-restacking method can be utilized bypassing the ordering of the lyotropic series. The former pathway exploits the memory effect of the LDH materials, *i.e.* the aptitude for the complete structural regeneration/rehydration of the heat-treated solids. During the preliminary calcination at high enough temperature the layered structure collapses with the removal of the interlayer anions, then, the introduction of new anions can become less constrained (Chibwe and Jones, 1989; Kuzmann et al., 2015). In the latter one, the delamination-restacking process that is, the hydrocalumite particles are exfoliated in certain solvents. From the prepared colloidal solution of the nanosheets, the LDH structures can be regained on removing the delaminating solvent, and during the recondensation the intercalation of extraneous anions become feasible (Wang and O'Hare, 2012; Pérez-Barrado et al., 2015). Furthermore, it was demonstrated quite recently that mechanochemical pretreatment could similarly help the introduction of the new anions among the layers. Milling caused fragmentation, and partial dehydration/delamination of the particles leading to complete amorphization (Wang et al., 2013; Olszówka et al., 2019) however, the layered framework could be successfully regained in aqueous solution also with new guest anions (Szabados et al., 2019b).

The intensifying interest in LDH − drug composites are originated from the numerous beneficial effects of the hybridization of the layered structure with significant organic anion exchange capability such as controlled and highly dispersed release from the interlamellar space, increased water solubility and hence bioavailability of the medicine molecules, economically friendly preparation and safe handling (Choy et al., 2017; Del Hoyo, 2007; Chatterjee et al., 2019). The strong electrostatic interaction between the host layers and the interlamellar anions lend for the LDH solids efficient protection potentials even for air/heat/light sensitive organic molecules like antioxidants (Kong et al., 2010) anti-cancer folate derivatives (Choy et al., 2004) or even DNA moieties (Choy et al., 1999). In addition, it is worthwhile to note that the LDH particles have individual escape mechanism from the acidic space of the lysosomes due to their basic character (Tyner et al., 2004). The combination of these valuable aspects with the multifarious composition, structure, morphology and biocompatibility of the LDH solids make these nanocomposites valuable platforms for several pharmacokinetic applications like drug monitoring, storing, delivering or even imaging.

The formulation of anti-inflammatory drugs by LDH particles is one of the most frequently and persistently researched field due to the large market demand of these medicines (Ambrogi et al., 2001; Khan et al., 2001). Another topic becoming more popular is the dermal application of these organic clays relying on their additional modifying effect related to the rheological attributes of semisolid materials (Chakraborty et al., 2014; Perioli et al., 2015). The Mg and Zn hydroxide based variants were successfully synthesized and applied for sunscreen stabilization and photoprotection avoiding the close contact between the sunscreen molecules and the skin (Perioli et al., 2006; Cursino et al., 2013). Several studies have also been published for their huge potential in transdermal antioxidant, anti-aging, anti-tumoral drug delivery and skin care treatments in cosmetics and pharmaceutical fields (Mosangi et al., 2016; Bastianini et al., 2018; Pagano et al., 2019). Moreover, the drug−polymer−LDH composites showed rapid dissolution and high enough mechanical robustness to utilize them as microneedle in clinical application (Yan et al., 2014). The above mentioned studies mainly used the direct anion exchange technique in the intercalation step; some even used other pre-introduced larger ions to pillar the layers and to facilitate the encapsulation of the drug molecules to be intercalated (Cursino et al., 2013). However, most of the published works dealing with the intercalation of non-steroidal anti-inflammatory drugs, like naproxen or diclofenac, also applied anion exchange, but there are some instances for the application of the co-precipitation method as well (listed in Table S1, "S" is the notation used in the Supporting Information).

In this contribution, our goal was to intercalate naproxen and diclofenac anions, into the interlamellar space of CaFe-layered double hydroxides by using and comparing four different intercalation techniques. The as-prepared solid composites were probed in detail studying their structural, textural, size, thermal and morphological properties, while their hydrogel forms were examined in *in vitro* drug release and *ex vivo* skin penetration tests as well. To the best of our knowledge, there is no report about skin penetration research of CaFe-LDH − drug preparations in spite of their lower toxicity and thus better biocompatibility than Mn(II), Co(II), Ni(II), Zn(II)-based or Al(III) incorporated LDH solids.

2. Experimental

2.1. Materials

The $Ca(NO_3)_2 \times 4H_2O$ and $Fe(NO_3)_3 \times 9H_2O$ were acquired from Reanal Private (HU). Anhydrous NaOH pellets, NaCl, Na_2HPO_4, K_2HPO_4

acetonitrile and methanol (both of HPLC grade) were purchased from VWR International (EU). The ethanol (pH. Eur.) and cyclohexanone was obtained from Molar Chemicals Company Ltd. (HU), while the sodium salt of diclofenac (or diclofenac sodium) from the Sigma-Aldrich (USA), the sodium salt of naproxen (or naproxen sodium) from the Zhejiang Charioteer Pharmaceutical Company Ltd. (CN) and the hydroxypropyl methylcellulose (Methocel® E4M) was delivered by the Colorcon Ltd. (UK). Concentrated NaOH (~19 M) stock solutions were produced by dissolving NaOH pellets and the exact concentration was calculated through accurate density analysis. The as-prepared liquids were filtered by 0.22 μm PTFE membrane using CO_2 trap to minimalize the carbonate content (Sipos et al., 2000). These liquids were diluted to obtain the 3 M NaOH stock solutions actually applied in the synthesis. All chemicals were of 99% + purity, and no further purification was required.

2.2. Synthesis and intercalation processes of the CaFe-LDH organic clays

The as-prepared LDH particles with nitrate as interlayer anions were synthesized following the relatively straightforward recipe of the co-precipitation route developed in our laboratory (Muráth et al., 2019); 7.1 cm^3 of aqueous NaOH solution (3 M) was added to 20 cm^3 of aqueous solution containing $Ca(NO_3)_2$ (0.3 M) and $Fe(NO_3)_3$ (0.15 M). The suspensions obtained were mechanically stirred (1000 rpm) under N_2 atmosphere at room temperature for 48 h reaching pH ~13. The precipitates were washed several times by distilled water (150 cm^3), collected on 0.45 μm filters and dried/stored at 70 °C under N_2 atmosphere.

Four techniques were investigated to intercalate/encapsulate naproxen and diclofenac anions among the LDH sheets; the dehydroxylation-rehydration method with diclofenac sodium was chosen to study the parameters of the successful intercalation in detail. Firstly, the dehydroxylation of CaFe-LDH samples was performed in a tube furnace under argon atmosphere at 400 °C for 2 h. The heat-treated solids (0.4 g) were stirred mechanically (1000 rpm) in an aqueous-ethanolic solution of diclofenac sodium (12 cm^3) under N_2. The temperature, the composition of the aqueous medium (distilled water/ethanol mixture) and the molar ratio of Fe(III) cations and diclofenac anions were systematically varied. After 7-day stirring, the as-prepared solids were collected on 0.45 μm filters and washed with the mixture of 25% v/v ethanol-water (60 cm^3). The drying and storing processes were the same as for the synthesis of the as-prepared LDH samples. The optimal intercalation parameters (1:1 Fe(III):diclofenac anion molar ratio, 25% v/v ethanol-water mixture, 25 °C) obtained were applied in the direct anion exchange, co-precipitation and mechanochemically-aided intercalation techniques as well.

During the direct anion-exchange method, the interlamellar nitrate anions were replaced by diclofenac anions with the mechanical stirring of the as-prepared LDH particles, 0.4 g solid material and 0.38 g diclofenac sodium were suspended and dissolved in 12 cm^3 water/ethanol mixed solvent, and was stirred for 7 days.

In the co-precipitation method, the aqueous solution of the base reagent was blended with ethanol and sodium salt of diclofenac was dissolved in it. The above-described aqueous calcium and nitrate solution (20 cm^3) was slowly added to the ethanol-water-NaOH-diclofenac mixture (7.1 cm^3), the NaOH concentration of the basic-ethanolic solution was 3 M and 0.95 g diclofenac sodium was dissolved in it. Finally, the precipitates were stirred for 7 days and washed with (150 cm^3) (25% v/v ethanol-water).

The mechanochemically-aided intercalation pathway consisted of two steps; first, the pristine CaFe−NO_3^--LDH particles were mechanically treated in a mixer mill (Retsch MM 400) operating with one-one grinding balls (stainless steel with ~8.2 cm^3 volume, diameter: 25 mm) and two grinding jars (stainless steel with 50 cm^3 inner volume). During the dry millings, the ball/sample mass ratio (60 g/0.3 g), the grinding frequency (12 Hz) and the time (30 min) were always fixed, and fully amorphous phases were gained verified by the X-ray diffractograms. In the second step, the process followed the method of the direct anion exchange; the milled solids (0.4 g) were stirred in the water-ethanol (12 cm^3) mixture of the dissolved diclofenac anions for 7 days. For the direct anion exchange, the co-precipitation and the mechanochemically-aided intercalation methods, the procedures of the washing, collecting, drying and storing were implemented similarly as described at the dehydroxylation-rehydration technique. For the intercalation of naproxen anions, all the already optimized parameters (25% v/v ethanol-water mixture, 25 °C, 1:1 Fe(III):naproxen anion molar ratio) were applied with replacing diclofenac sodium by the naproxen salt.

2.3. Preparation of the hydrogels with and without LDH particles

The LDH solids (0.1 g) were dispersed thoroughly in the mixture of 4 g distilled water and 0.5 g ethanol using ultrasonic bath for 5 min. The hydrogels were prepared separately, 0.35 g HPMC (hydroxypropyl methylcellulose) were stirred in 5.05 g distilled water, the hydrogels start forming within 1 h, and then, it was blended *via* intense stirring (500 rpm) with the homogenized dispersion of LDH samples. For the control samples, 0.04 g of diclofenac or naproxen were dissolved in the already described ethanol-water mixture, and added to the hydrogels using the already described procedure.

The pH values of hydrogels were determined by a testo 206 pH meter and are reported in Table 1. The CaFe-LDH − gel systems proved to be strongly alkaline compared to the control samples owing to the high basicity of the calcium hydroxide components. Although, this significantly limited the potential application of these hydrogels in the pharmaceutical or cosmetic fields, with a simple neutralizing post-treatment, Mosangi et al. (2016) demonstrated that the pH of ZnAl-LDH − gels could be reduced easily to reach the ~5.6 value, which is the pH of the healthy skin. Nevertheless, the increased acidity can induce the partial dissolution of metal hydroxide parts, and hence, the uncontrolled release of intercalated anions. Therefore we refrained the use of acid treatment, in order to see the effect of the interlayer space on the storage/dose of diclofenac and naproxen anions more cleanly and clearly.

The drug content of the gels were determined by ultra-high performance liquid chromatography (UHPLC), and their LDH contents were 1% w/w. For the measurements, 100 mg gel was dissolved in 10 cm^3 of citric acid-methanol mixture (3 cm^3 0.1 M of citric acid aqueous solution and 7 cm^3 of methanol), the suspensions obtained were treated on an orbital shaker for 10 min with 500 rpm speed. The dissolved gels were purified by 0.22 μm syringe filters and the clear liquids were analysed on a Shimadzu Nexera X2 liquid chromatograph (Table 1).

For registering the diclofenac content, the chromatograph was operated with 50 mm × 2.1 mm × 2.6 μm C18 reverse-phase column

Table 1
The measured pH and drug content (calculated for the anionic forms) values of the 1% w/w CaFe-LDH containing hydrogels and the BET specific surface areas of initial organic clays.

Sample	pH	Drug content (% w/w)	BET (m^2/g)
control diclofenac	7.38	0.37	–
co-precipitation LDH − diclofenac	11.46	0.46	22
direct anion exchange LDH − diclofenac	11.45	0.33	28
dehydroxylation-rehydration LDH − diclofenac	11.39	0.55	8
mechanochemically-aided intercalation LDH − diclofenac	11.26	0.26	18
control naproxen	8.50	0.36	–
co-precipitation LDH − naproxen	11.65	0.28	40
direct anion exchange LDH − naproxen	11.70	0.36	43
dehydroxylation-rehydration LDH − naproxen	11.68	0.41	23
mechanochemically-aided intercalation LDH − naproxen	11.51	0.34	41

(Phenomenex Kinetex C18), and the data were collected with a diode array detector working at 274 nm. The mobile phase was 64:36 methanol:sodium dihydrogen phosphate buffer solution (pH 2.5) in isocratic elution, while the flow rate was 0.5 cm^3/min and the injection volume was 3 μl. The temperature of the column was set to 40 °C, and the retention time of the diclofenac was around 1.5 min. The naproxen content was determined similarly, but the applied column was a Thermo Scientific Hypersil Gold C18 with 100 mm × 2.1 mm × 1.9 μm dimensions, the data collection was performed at 230 nm, and the retention time of the analyte was 2.1 min. The mobile phase was comprised of sodium dihydrogen phosphate buffer solution (pH 2.5) and acetonitrile in 58:42 volume ratio.

2.4. Applied techniques for structural characterization

As main method for verifying the success of the LDH synthesis, the intercalation processes and for probing the structural changes occurred, the powder X-ray diffractometry (XRD) patterns were recorded in the Θ = 3–60° range with 4°/min scan speed using $Cu_{K\alpha}$ (λ = 1.5418 Å) radiation on a Rigaku Miniflex II instrument (equipped with a scintillation detector, Ni foil *Kβ* filter operating at 30 kV and 15 mA, in continuous mode with step width of 0.02° 2θ). On the normalized diffractograms, the reflections were assigned with the help of the JCPDS−ICDD (Joint Committee of Powder Diffraction Standards − International Centre for Diffraction Data) database. The interatomic distances were calculated with the Bragg equation. The coherently scattering domain sizes of CaFe-LDH particles (the average crystal thicknesses from the layers constructed into each other) were estimated by the Scherrer equation fitting Gaussian curves on the first reflections of the LDH phases using 0.9 shape factor.

To investigate the presence and linking of the drug molecules and the structural peculiarity of the LDH composites, the samples were studied by Fourier-transform Raman and infrared spectroscopies. The former was a Thermo Scientific DXR Raman microscope equipped with diode laser and CCD camera. The magnitude of optics was 10× and the aperture was 25 μm. The spectra were recorded with 780 nm laser at 10 and 24 mW power level accumulating 16 scans for 6 s exposure time including fluorescence and cosmic ray corrections. The normalized curves were studied in the 1800–180 cm^{-1} wavenumber range. The Fourier-transform infrared spectrophotometer worked (JASCO FT/IR-4700) with 4 cm^{-1} resolution accumulating 256 scans and equipped with ZnSe ATR accessory and DTGS detector. The structural properties of solids were mapped in the range of 4000–600 cm^{-1} on the normalized curves.

In the 30–900 °C temperature range, the thermal behaviour of the hybridized CaFe-LDHs focusing on the thermal stabilities of the intercalated drug molecules were investigated with a Setaram Labsys TGA-DTA 1600 derivatograph working under constant flow (60 ml/min) of air at 5 °C/min heating rate. For the analysis, 20–25 mg of the materials were taken into high-purity alpha alumina crucibles.

A Malvern NanoZS dynamic light scattering apparatus (4 mW helium-neon laser light source, λ = 633 nm) was applied to determinate the zeta potential (for surface charge), solvodynamic diameters and heterogeneity in particle sizes of pristine and drug-intercalated LDH solids. By 2 h ultrasonic pre-treatment, dispersions with 0.1 g/dm^3 concentration were prepared in cyclohexanone medium.

In order to evaluate the area and heterogeneity in sizes of the LDH particles dispersed in hydrogels, the preparations were pressed between glass slides and probed by Leica DM6 B digital light microscope equipped with Leica DFC 7000 T camera. The magnification was 10×, and the images were processed by the LAS X software package.

The specific surface area of organic LDH samples were determined by N_2 adsorption-desorption techniques on a Quantachrome NOVA 3000e instrument. Before the measurement, the samples were degassed at 110 °C for 2 h to remove surface adsorbates and the area values were calculated from the adsorption branches using the Brunnauer−Emmett−Teller (BET) equation.

The morphologies of LDH particles were investigated by scanning electron microscopy (SEM, Hitachi S-4700) at different magnifications and acceleration voltages. The elemental analysis was done by energy dispersive X-ray (EDX) analyzer accessory coupled to the microscope (Röntec QX2 spectrometer equipped with Be window).

2.5. Used apparatus of drug liberation tests

To model and study the *in vitro* drug diffusion from the LDH samples with intercalated diclofenac and naproxen anions, a vertical Franz diffusion set-up was utilized including a transdermal diffusion cells with Hanson Microette plus and Logan automated dry heating system. The donor chambers (~1.8 ml) were filled with freshly prepared hydrogels in varied amounts (between 240 and 310 mg). The acceptor phase was phosphate buffer solution (pH 7.4 ± 0.2, stirring rate 400 rpm, 7 ml) thermostated to the surface temperature of the human skin (32 ± 0.5 °C). The donor and the receptor chamber with the acceptor phase was separated by a synthetic mixed cellulose ester membrane, PORAFIL CM® with 0.45 μm pore size. All diffusion tests were repeated six times with the relevant hydrogel−LDH systems. The quantity of the permeated diclofenac and naproxen anions was followed by the already described ultra-high performance liquid chromatography measurements.

The transdermal way of intercalated anions were visualized by through skin penetration tests on separated Caucasian female abdominal skin by Raman microscopy analysis. The human skin was obtained from the Department of Dermatology and Allergology, University of Szeged, the *ex vivo* studies did not require the consent of the patient and ethical permission according to the Act CLIV of 1997 on health, Section 210/A in Hungary. The ethical committee of the University of Szeged, Albert Szent-Györgyi Clinical Centre was briefed on the *ex vivo* penetration tests (human investigation review board license number: 83/2008). The Thermo Scientific DXR Raman microscope was operated with 780 nm laser light at 24 mW power level accumulating 16 scans with 2 s exposure time and 25 μm aperture of the pinhole for each spectrum. The chemical scanning was performed on a 200 × 1000 μm area with 50 μm vertically and horizontally step size collecting 105 spectra and for making the correlation maps untreated human skin was applied. The evaluation of data was done by the OMNIC for Dispersive Raman 8.2 software package. The human skin was stored at −21 °C and sectioned (−32 °C blade temperature) by a Leica CM1950 cryostat system onto aluminium-coated slides. On 2000 × 1000 μm area, 250 mg LDH − gel was dispersed and the skin was placed onto sterile cotton wool wetted with physiological saline solution. After 24 h treatment, the gels were removed just before the Raman microscopy analysis.

3. Results and discussion

3.1. X-ray diffractometry investigations

The development of the intercalation processes was started by the dehydroxylation-rehydration method; this is the most frequently used way for introducing larger organic anions in-between the interlamellar space, because of the absence of other competitor intercalating anions in appreciable amount. While, the diffractogram of the as-prepared nitrate-containing CaFe-LDH (JCPDS card: 48–0065) did not show any sign of calcite phase generation (Fig. 1), after the heat treatment, a weak signal of $CaCO_3$ (JCPDS#47–1743) phase was observed next to the reflections of $Ca_2Fe_2O_5$, evolved (JCPDS#47–1744) from the complete dehydration of the LDH (Fig. S1). Since, calcination was performed under argon atmosphere, the formation of calcite particles in minute amount could originate from the presence of surface-adsorbed CO_2 molecules in larger quantities, as the infrared spectra attested (Fig. 3). The noticeable growth in the baseline stemmed from the fluorescence of iron atoms and the presence of amorphous particles.

As the first step, the composition of the applied aqueous media was

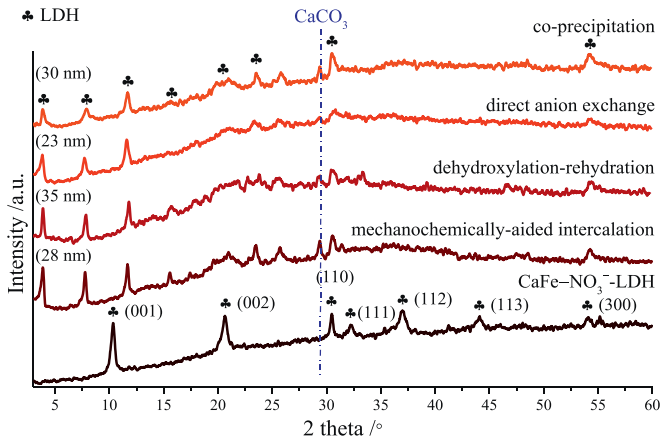

Fig. 1. X-ray diffractograms of the as-prepared LDH and the composites synthesized by the *v*arious intercalation techniques (1:1 Fe(III):diclofenac anion molar ratio, 25% v/v ethanol-water mixture, 25 °C).

varied in wide range from the 87.5% v/v to the 25% v/v ethanol-water mixture; this step proved to be necessary because of the poor solubility of naproxen and diclofenac sodium salts even in highly alkaline (3 M NaOH) environment. The most intense basal reflections of the LDH phase were shifted clearly to the lower 2θ position (the first one to around 3.9°), and these signals preserved their periodic arrangement as a direct evidence for the success intercalation of the diclofenac anions (Fig. S1). However, the increased volume of the ethanol aided the dissolution of drugs, it inhibited the generation of the LDH phase, less layers could attached to each other. The calculated crystal thickness (35 nm) was the highest at the lowest ethanol amount.

As further steps, the effect of the temperature applied and the Fe(III): diclofenac anion molar ratio were investigated in detail. The increasing temperatures generally help the formation of hydrocalumites because of the exothermic dissolution of calcium hydroxide parts (Szabados et al., 2016). The reflections of the diclofenac or the nitrate anion containing LDH phases could not be observed at higher temperature (Fig. S2). As a possible explanation, the diclofenac anions might form complexes with the calcium and/or iron cations (several new reflections were observed between 20 and 45° 2θ) at elevated temperature and hence inhibited the generation of the CaFe-LDH. Theoretically, the maximum amounts of the intercalated diclofenac anions follow the content of incorporated Fe (III) ions into the structure of portlandite, but the adsorption of molecules on the external surface and the intercalation of other anions like hydroxide or even ethoxide anions can modify this ratio. Therefore, our examinations were supplemented by tests with varied Fe(III):diclofenac anion molar ratios (Fig. S3). The thickest crystals were obtained at the initial 1:1 Fe(III):diclofenac molar ratio, but the diffractograms attested successful LDH formation at higher and even at lower molar ratios. Moreover for the use of the lower diclofenac amount, the peak shoulder at ~11.4° 2θ could induce the collateral intercalation of hydroxide/carbonate anions.

The 25% v/v ethanol-water solvent mixture, room temperature stirring and 1:1 Fe(III):diclofenac anion molar ratio were identified as the optimal parameters for the dehydroxylation-rehydration method. These conditions were applied successfully for co-precipitation, direct anion exchange and mechanochemically-aided intercalation of diclofenac anions as well (Fig. 1). For all cases, the measured basal distances (sum of the interlamellar space and layer thickness) were increased from the initial 0.85 nm, characteristic for the nitrate anions ruled interlamellar space (Szabados et al., 2018), up to 2.27–2.3 nm values due to the successfully intercalated large organic anions in the interlayer gallery (Table S2). Beside the shifted basal and the several new reflections (unsuccessful assignation as likely secondary products) presumably originating from the modified crystal structure, the (110) and (300) non-basal ones could be observed in position characterized by the 0.582–0.586 nm *a* lattice parameters (average metal cation–cation distance) remained largely unchanged indicating the presence/integrity of the layers (Gastuche et al., 1967). The work with the naproxen anions showed similar results (Fig. 2, Table S2). By using all techniques, the intercalation of anions could be achieved, the basal distances increased (1.9–1.94 nm); however, some calcite was also formed. Interestingly, the anion content of the LDH solids (Table 1) were relatively in good correlation with the values (between 23 and 35 nm) of the calculated crystal thicknesses, especially for the work with naproxen. For both anions, the dehydroxylation-rehydration method resulted in particles with the highest drug content as well as the largest average crystal thicknesses.

3.2. Fourier-transform infrared and Raman spectroscopy studies

The infrared spectra of the hybridized CaFe-LDH composites showed both the characteristic absorption bands of the organic anions and the layered hydroxide framework. Between 3000 and 3600 cm^{-1}, the signals of M − OH band stretch and hydroxyl groups in the hydrogen bonding network, at 1415 cm^{-1}, the band of reversibly surface-adsorbed CO_2 molecules could be observed clearly in the LDH samples (Fig. 3A, B). Under 1600 cm^{-1}, the intense C − C and C − H stretching vibrations of aromatic rings demonstrated the presence of organic anions, while the shifts of the carboxylate vibrations (symmetric one from 1397 to 1383 cm^{-1} for the diclofenac and asymmetric one from 1583 to 1556 cm^{-1} for the naproxen intercalation (Fini et al., 2010; Sharma et al., 2013) are indicated the strong electrostatic interaction between the anions and the positively charged layers. The displacement of the asymmetric (from 1572 to 1551 cm^{-1}) and symmetric (from 1409 to 1391 cm^{-1}) carboxylate stretching vibrations for the work with diclofenac and naproxen anions, respectively, can be also observed. However, their identification is pretty complicated due to the intense bands of the diclofenac ring vibrations at around 1587 and 1558 cm^{-1} and the likely presence of the pseudopolymorphic forms of the naproxen sodium salt resulting in large fluctuations in the symmetric vibration of the carboxylic groups (Fini et al., 2010; Jamrógiewicz et al., 2021). The absence of the intense ν_3 symmetric stretch of nitrate groups (at 1345 cm^{-1}) in the LDH − drug composites also confirmed the successful replacement of initial nitrates by the organic anions (Renaudin et al., 1999).

The Raman microscopic probe of LDH composites verified the structural attributes derived from infrared measurements (Fig. S4A, B), the C − H, C − C and C − O vibrations of the organic molecules were

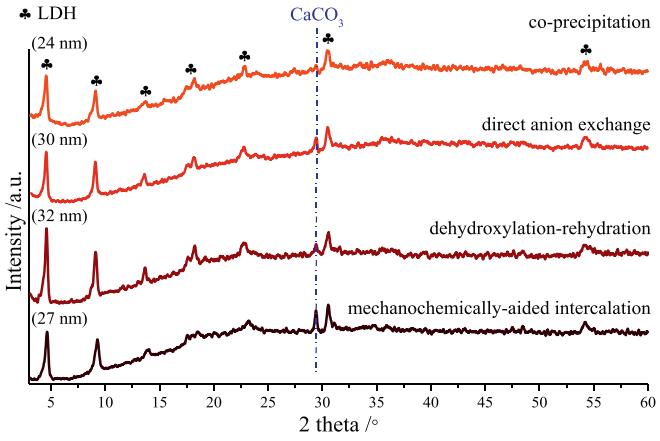

Fig. 2. X-ray diffractometry patterns of LDH composites prepared by the different techniques (1:1 Fe(III):naproxen anion molar ratio, 25% v/v ethanol-water mixture and 25 °C).

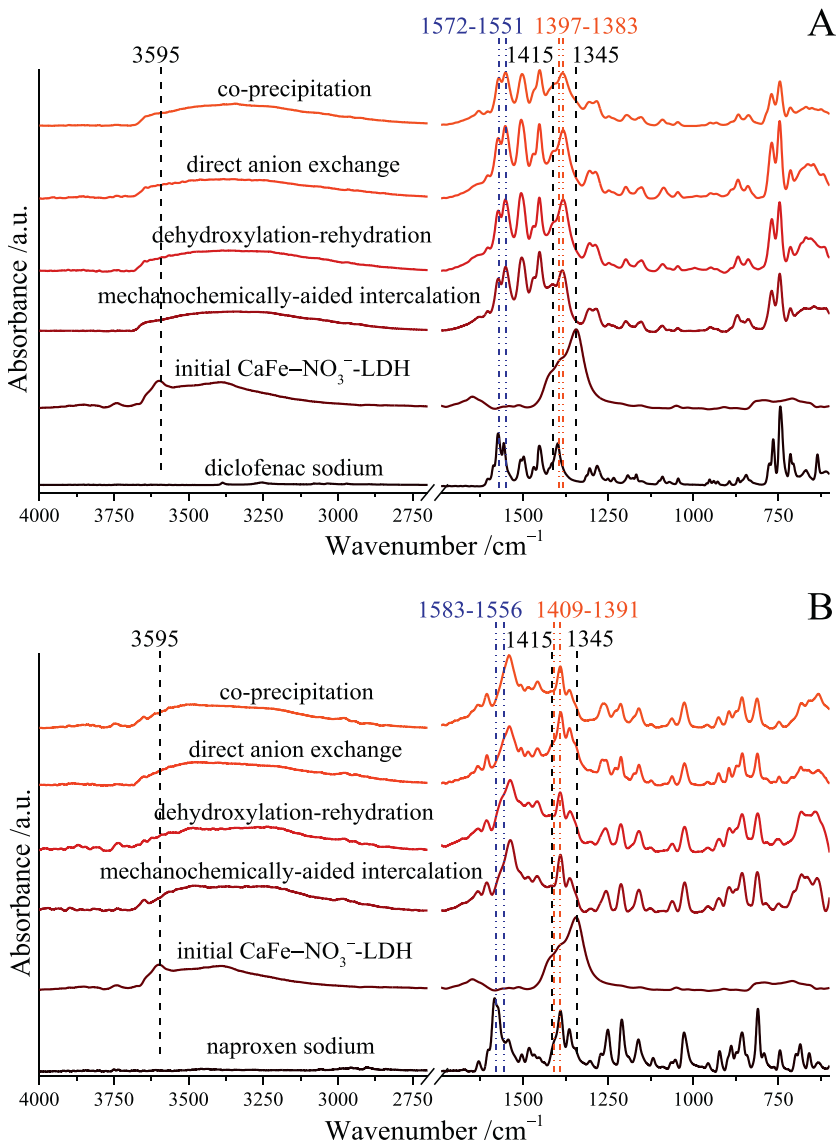

Fig. 3. Infrared spectra of LDH samples with intercalated diclofenac (A) and naproxen (B) anions and those of the initial LDH and the starting drugs.

easily observable in the 1700–500 cm^{-1} region (Fini et al., 2010; Saji et al., 2020). In as-prepared CaFe-LDH sample, the Raman active vibrations of interlayer nitrate groups at 1055 and 715 cm^{-1} were recorded with the stronger lattice vibration of Ca – O – Fe chains around 510 and 355 cm^{-1} as well (Al-Jaberi et al., 2015). However, these signals were not or just hardly observed, respectively, in the organo-LDH solids. The microscopic character of the Raman analysis meant surface sensitive data from the solids measured, and the surface adsorption of initial drug molecules could mask the vibration of LDH framework. Although, the intense reflections of the naproxen/diclofenac sodium were not observed in the corresponding diffractograms (Fig. S5), their presence was likely, in spite of the applied intense washing procedure. EDX analysis indicated sodium atoms in minute amount (Fig. S6), and the weak vibrations under 400 cm^{-1} could be attributed to the Na – O bonds (Saji et al., 2020). Finally, the absence of shift in the carboxylate stretching bands could also be interpretable by the multilayer adsorption of drug molecules on the external surface of LDH particles.

3.3. Electron microscopic, thermal and particle size analysis

Since the XRD, FT-IR and Raman spectroscopies did not indicate significant disparities regarding the outcome of intercalation of drug molecules, the results of electron microscopy as well as the thermal measurements are demonstrated exclusively on the solids prepared by the dehydroxylation-rehydration method.

The electron microscopy images displayed the lamellar arrangement of distorted hexagonal-shaped particles between 400 and 1000 nm (Fig. 4). The absence of regular hexagons can be explained by the crystallization inhibition of the surface-adsorbed organic molecules in the crystal growth step. The chloride content of diclofenac molecules made possible the visual detection of the spatial distribution of organic anions in the LDH particles. The chloride, as well as the calcium and iron ions were placed uniformly, no segregation were observed (Fig. S7A, B, C); this is an indirect evidence for the complete dispersion of drug molecules on the internal and the outer surfaces, and for the successful LDH formation ruling out the generation of unidentified secondary phases containing exclusively Fe or Ca ions.

The composites showed the characteristic mass losses of the LDH structure (Forano et al., 2006) merged with the mineralization of

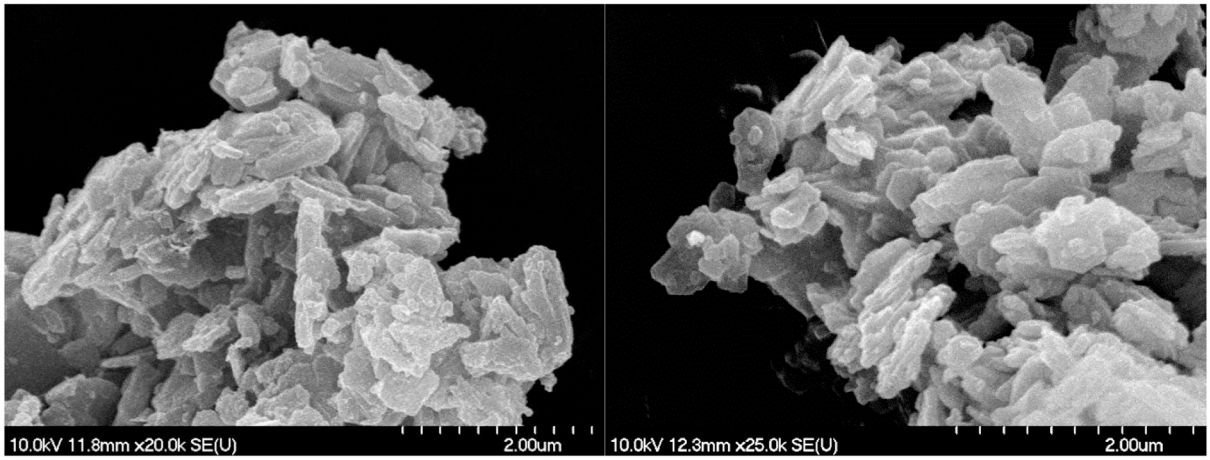

Fig. 4. SEM images of the hybridized CaFe-LDH solids (left – diclofenac and right – naproxen anion-containing LDH samples).

intercalated drug molecules (Fig. 5). The interpretation of thermal behaviour was supported by thermogravimetric curves of the as-prepared nitrate-containing CaFe-LDH and the diclofenac and naproxen sodium salts under the same measuring conditions (Fig. S8). The physically adsorbed water molecules from the external surface departed first, until 150 °C causing 8–11% mass loss, and it was followed by the evaporation of interlayer water molecules. This step could be connected to only one mass loss peak (around 10%) with maximum at 245 °C for the as-prepared CaFe−NO_3-LDH; however, it was separated into two processes with maxima at 180 (2–3%) and 250–260 °C (4–5%) for the drug-intercalated LDH particles. In the hydrocalumites, the extra coordination sites in the coordination sphere of the Ca(II) ions can be occupied by water as well as ethanol molecules (Renaudin et al., 1999; Bugris et al., 2013), which can explain their discontinuous evaporation.

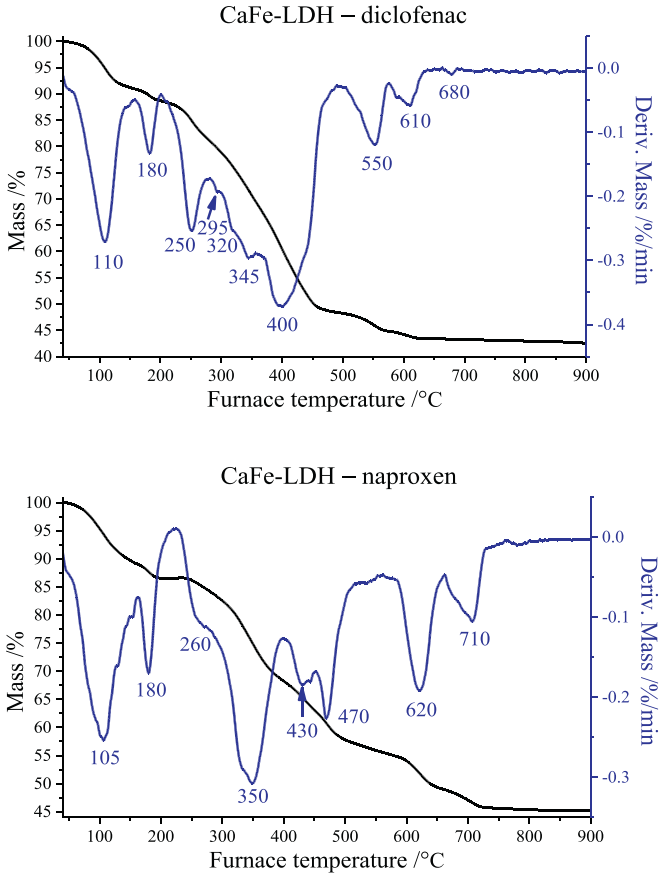

Fig. 5. Thermogravimetric curves for the diclofenac and naproxen anion-intercalated CaFe-LDH samples.

At higher temperatures, the mass losses attributed to the dehydration/dehydroxylation/decomposition of the metal hydroxide parts and the diclofenac or the naproxen anions were poorly separated. For the diclofenac−LDH system, a large (~30%) mass loss between 290 and 500 °C was observed derived from the simultaneous mineralization of the diclofenac anions and the water loss from the Ca/Fe − OH moieties. At 550 °C (5%), 610 °C (2%), and 680 °C (under 1%) were attributed to the decomposition of the organic groups further and those of the *in situ* (from the CO_2 content of the furnace air of the thermogravimetric analyzer) and *ex situ* evolved calcite phases. Bands between 300 and 400 °C indicated the dehydroxylation of the LDH component of the naproxen anion−CaFe-LDH composite and the decomposition of the organic anions (14%), while around 430 and 470 °C the further mineralization of drug molecules (12%) took place in remarkable amounts. The mass losses at around 620 (7%) and 710 °C (4.5%) could be associated to the decomposition of the residual organic parts (decarbonization) and calcite particles.

The intercalation of the drug anions could significantly modify the thermal attributes of the initial LDH structure. The closed environment of the interlamellar space could protect thermally the diclofenac anions shifting the maxima of the decomposition from 285 °C to around 320 °C. However, the intercalated naproxen anions attested faster mineralization, it occurred presumably most intensely around 350 °C instead of the 380 °C of the pure naproxen sodium, and for both solids, the dehydroxylation of metal hydroxides also started at lower temperatures compared to value of the as-prepared CaFe-LDH samples (around 515 °C – decomposition of nitrate anions and the Ca/Fe − OH parts). The infrared spectra of the heat-treated samples (25–400 °C, 1 h) verified the results derived from the thermogravimetric curves: the LDH composites were intact until the 200 °C and underwent gradual structural decomposition, dehydroxylation up to 400 °C (Fig. S9). The C − O, C − H and C − C vibrations of carboxylate and aromatic ring groups disappeared near completely until the 350 °C heat treatment for both LDH composites, while the pure diclofenac salt and sodium naproxen disintegrated in the 250–300 °C and 350–400 °C temperature ranges, respectively.

By the dynamic light scattering technique, the as-prepared and the drug-intercalated LDH solids were analysed choosing cyclohexanone as the fluid medium to avoid the delamination of the particles and create stable, non-settling dispersions (Szabados et al., 2019a). The number-weighed size distribution curves of samples showed largely unimodal characters (Fig. S10), and the polydispersity indices changed between

0.13 and 0.46 indicating slightly polydisperse systems (Table S2). However, direct tendency was not observed between the calculated average predominant solvodynamic diameters and the types of preparation techniques applied. The aggregation of LDH particles were clearly enhanced by the intercalation of the naproxen and the diclofenac anions. The size of the aggregated organoclays grew from ~250 nm (as-prepared CaFe−NO_3^--LDH) up to even >3000 nm, presumably because of the evolution of a hydrogen-bonded network and attractive electrostatic forces between the surface adsorbed drug molecules and the metal hydroxide layers. Zeta potential measurements revealed negatively charged particles in spite of the generally measured positive values at nitrate or carbonate intercalated Mg-based LDH composites (Zhou et al., 2012; Abdellaoui et al., 2019) revealing two responsible phenomena. One is the strong affinity of the calcium hydroxide based LDH variants to the carbonate ions originating from airborne CO_2, the second is the presence of surface-adsorbed organic anions in remarkable amount (Xu et al., 2008). Interestingly, the intercalation of the naproxen anions resulted in less negatively-charged surfaces with smaller electrostatic repulsion, and, therefore, the agglomeration of particles got more intensified.

The attractive/repulsive forces between the clay particles and the hydroxypropyl methylcellulose molecules, the applied mass transfer and the not fully homogeneous distribution of spots with slightly different pH environment have serious influence on the aggregation tendencies. Therefore, the sizes and the heterogeneity of sizes of LDH particles dispersed in hydrogels were also analysed visually in transmitted light. By using image analysis software, the area of dark objects (solid grains) were used to calculate the size distribution parameters. The majority (32–54%) of the particles had areas between 5 and 10 μm^2, but the applied intercalation techniques as the quality of the interlayered anions had significant influence on the distribution of LDH grains (Fig. 6). For the diclofenac−LDH samples prepared by co-precipitation or the mechanochemically-aided ways, the amounts of particles with 1–10 μm^2 and 10–50 μm^2 area remained under ~40–40%, while these values were around 80–75% and 19–22%, respectively, for the intercalations by direct anion exchange or the dehydroxylation-rehydration method. In the highest amount, the particles were moved toward the upper sizes (≥50 μm^2 area) for the co-precipitated (~20%) and mechanochemically-prepared (~11%) diclofenac−LDH. Interestingly, similar heterogeneity regarding the size distribution in the naproxen anion-encapsulated LDH − hydrogels was not detected (Fig. S11) for any sample, irrespective to the method of synthesis. The main part of particles (almost more than 60%) had the area between 1 and 10 μm^2, and the amount of the largest particles (≥50 μm^2) remained under 8%.

3.4. Drug liberation and skin penetration studies

The *in vitro* comparative release tests were performed in vertical Franz diffusion cells using synthetic mixed cellulose ester membranes and drug anion-containing LDH − gels in the donor chamber. The permeation of diclofenac and naproxen anions into the membranes occurred by passive diffusion mainly directed by gravity and the concentration gradients toward the phosphate buffer acceptor phase in the receptor chamber. The cumulative mass values of the diffused drugs were similar, altered in the range of 600–1000 μg/cm^2 after 24 h, and the liberation of organic molecules could be successfully lengthened by encapsulating them into the LDH particles compared to the results obtained with the control gels (Fig. 7). The burst release of drug molecules could be observed for several preparations, and more intensely for the naproxen anions, presumably, due to their higher solubility in the aqueous media that of the diclofenac anions. However, the intercalation by the co-precipitation technique could diminish it efficiently in both

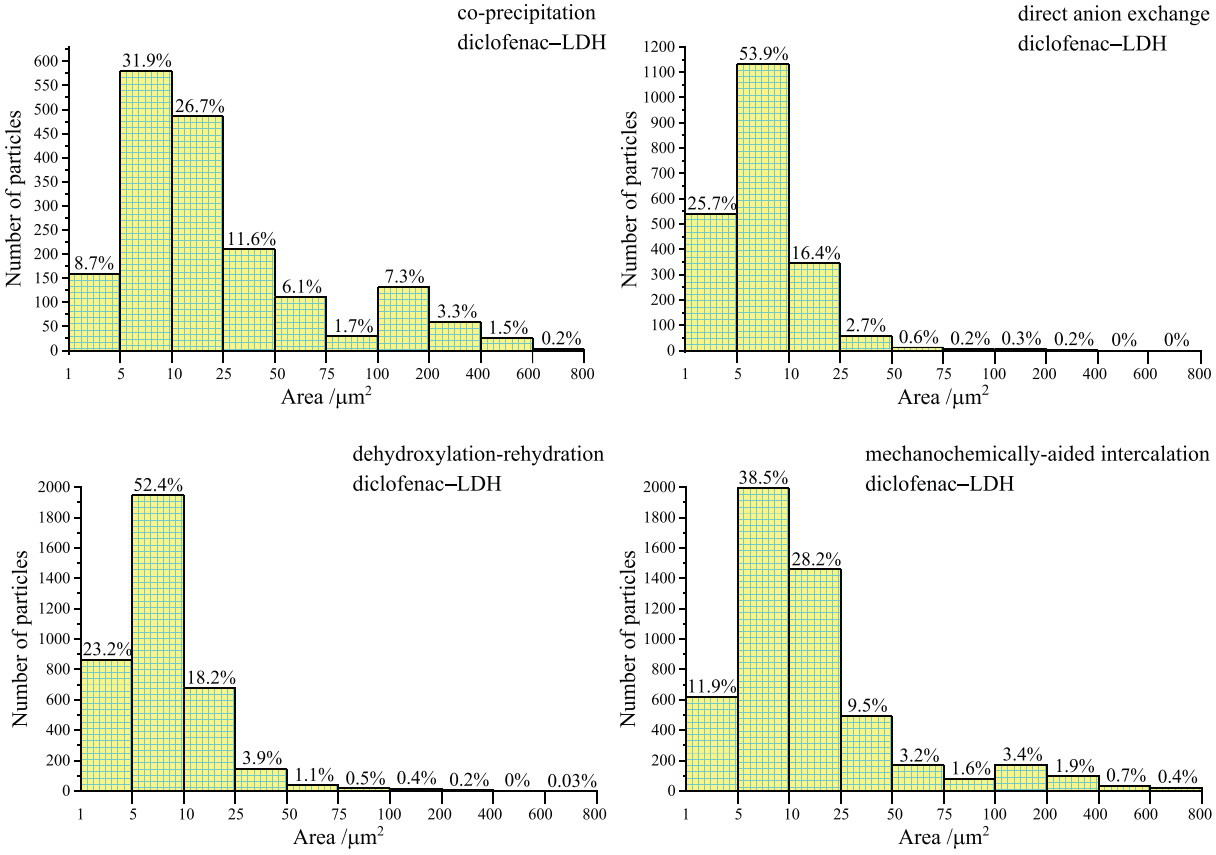

Fig. 6. Particle size distribution histograms of the diclofenac anion-intercalated CaFe-hydrocalumites dispersed in hydrogels.

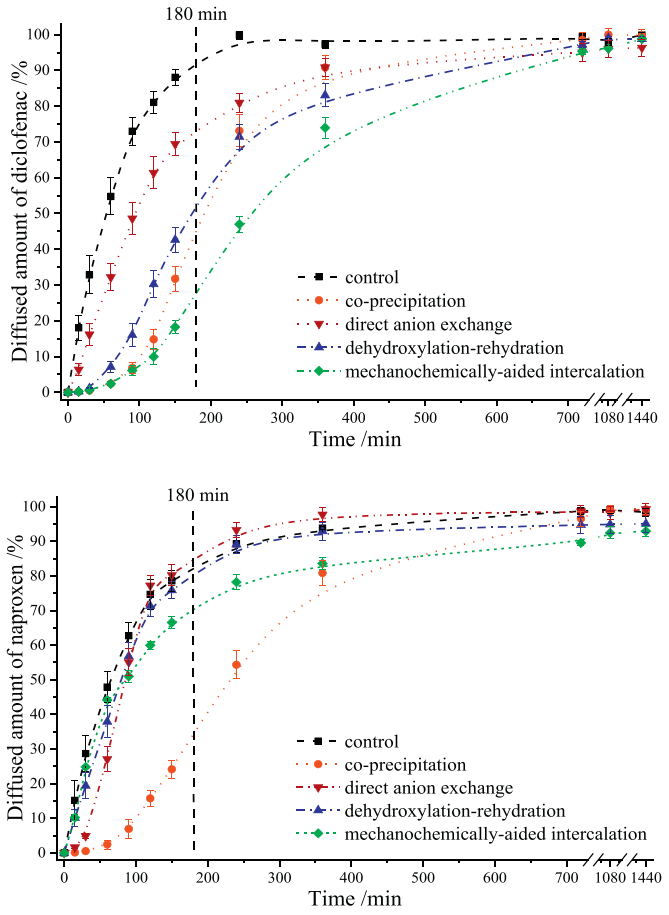

Fig. 7. Drug release studies of the diclofenac and naproxen anion-containing LDH – gels (at zero minute the points demonstrate the absence of drug molecules).

systems. The main amount of drug molecules could reach the receptor chamber within 3–6 h, but significant differences were observed regarding the encapsulation methods applied. For both anions, the co-precipitation and the mechanochemically-aided intercalation techniques proved to be the most suitable to prepare organo-CaFe-LDH composites with most prolonged drug liberation, the direct anion exchange and the dehydroxylation-rehydration method showed lower retention potential. The amount of released diclofenac molecules were systematically over 96% after 24 h, but these values remained under 95 and 93% for the naproxen intercalation by the dehydroxylation-rehydration and the mechanochemically-aided ways, respectively.

The kinetics of the drug release from the LDH composites are generally preceded by several steps; the dissolution of adsorbed anions from the external surface (explaining the burst effects), the weathering of LDH particles and the ion-exchange reaction of the interlamellar space, here, between the hydroxide ions in the gel matrix and/or phosphate anions from the acceptor phase (salt components of the sweat/saline solution in *ex vivo* tests) and the interlayer organic anions (Mosangi et al., 2016; Yang et al., 2003; Bi et al., 2014). Moreover, the solubility and diffusion of drug molecules in the hydroxypropyl methylcellulose matrix applied, the geometry of the measuring systems, the quality of membranes and the mass transfer properties also behave as key parameters (Siepmann and Peppas, 2001). The term diffusion is frequently used in respect of the movement of drug molecules along the LDH particles and the solution layer surrounding them describing the half of step of the ion exchange, thus the comparison of the literature findings is extremely complicated. One of the most applied model to describe the kinetics of the drug release from LDH – drug composites is the Korsmeyer–Peppas or Ritger–Peppas equation; $\%D = M_t/M_\infty * 100 = k*t^n$, where M_t and M_∞ are the cumulative drug released in time t and infinite time, k and n are the kinetic release rate coefficient (including the setup characteristics of the measuring system) and the release exponent typifying the mechanism of the drug liberation, respectively (Costa and Lobo, 2001; Siepmann and Peppas, 2001; Bruschi, 2015). If n remained under 0.45–0.5, the rate determining step of the drug release is the Fickian diffusion (if $n = 0.5$ it is called Higuchi model). Values from 0.5 to 0.89–1 correspond to the non-Fickian diffusion, in this anomalous transport the dissolution/erosion of LDH solids, ion exchange processes and the diffusion of the drug molecules jointly determine the kinetic of the liberation. When $n > 0.89–1$, the drug release is driven by the weathering kinetics of LDH particles (Rojas et al., 2014; Khan et al., 2008; Li et al., 2009; Salguero et al., 2020).

The values of R^2 linear correlation coefficients and standard deviations were in the acceptable range regarding that non-uniform sizes and spatial arrangements of solids were detected in the gel matrix (Table 2). The kinetic release constants remained under the values measured in the control hydrogels for both drugs, meanwhile the n parameters showed large fluctuations depended on the quality of interlamellar anions and the way of the encapsulation. In all cases, the liberation was nearly complete after 18–24 h, the drug releases were led exclusively by surface reaction controlled processes, values of n were between 0.93 and 2.34. Except the case of the naproxen intercalation with the dehydroxylation-rehydration and the mechanochemically-aided techniques, where n described the anomalous transport case. Interestingly, it was in parallel with the measurements of solvodynamic diameters of LDH particles (Table S2), the largest sizes were observed for these cases. Thicker sizes and thus higher drug contents on their outer surfaces (resulted in enhanced burst effect) could be responsible for the lower n exponents and for the increased kinetic release constants accompanied by faster, but not complete disintegration of the particles.

When the LDH solids suffered close to spontaneous dissolution in acidic environment, the diffusion and solubility of drug molecules turned into the key factors. In neutral or alkaline aqueous media, the process of the ion exchange mainly determined the rate of drug release from the LDH composites due to the low solubility/relative large stability of the metal hydroxide layers (Tyner et al., 2004; Rojas et al., 2014), and values of n remain under 1 as it was calculated for the common Mg- and Zn-based diclofenac/naproxen containing LDH composites (Table S1). The hydrocalumites have enhanced weathering character because of the moderate water solubility of calcium hydroxide moieties, while the increasing concentration of hydroxide ions did not

Table 2
Korsmeyer–Peppas kinetic data and fitting parameters of drug release from the preparations.

Sample	n	k (%/min^n)	R^2
control diclofenac	0.64 ± 0.06	3.789 ± 1.22	0.961 ± 0.005
co-precipitation LDH – diclofenac	2.23 ± 0.07	$3.5 \times 10^{-4} \pm 1.1 \times 10^{-4}$	0.993 ± 0.001
direct anion exchange LDH – diclofenac	0.93 ± 0.05	0.665 ± 0.189	0.966 ± 0.006
dehydroxylation-rehydration LDH – diclofenac	2.13 ± 0.04	$9.4 \times 10^{-4} \pm 2.8 \times 10^{-4}$	0.985 ± 0.004
mechanochemically-aided intercalation LDH – diclofenac	1.96 ± 0.02	$8.7 \times 10^{-4} \pm 2 \times 10^{-5}$	0.995 ± 0.002
control naproxen	0.67 ± 0.09	3.103 ± 0.821	0.961 ± 0.009
co-precipitation LDH – naproxen	2.34 ± 0.13	$2.3 \times 10^{-4} \pm 8 \times 10^{-5}$	0.994 ± 0.004
direct anion exchange LDH – naproxen	1.61 ± 0.04	0.027 ± 0.006	0.934 ± 0.004
dehydroxylation-rehydration LDH – naproxen	0.84 ± 0.07	1.22 ± 0.445	0.972 ± 0.002
mechanochemically-aided intercalation LDH – naproxen	0.72 ± 0.03	1.931 ± 0.275	0.938 ± 0.007

harm the solubility of released anions, hence almost complete drug liberation could be observed within 18 h in our all cases. The speeds of the weathering and the ion-exchange courses of CaFe-LDH solids coincided well in the alkaline environment (Xu et al., 2015; Zhou et al., 2015; Jaberi et al., 2019). The low concentration of foreign hydroxide ions in the early stage (originated from the decomposition of the Ca − OH parts), of the phosphate anions permeated through the membrane from the acceptor phase and the relative fast dissolution meant limited reintercalation in the disappearing interlamellar galleries. In addition, the cellulose chains also caused some solubility and solvent transport decrease for the LDH particles, naproxen and diclofenac anions in the hydrogel matrix (resulting in slightly distinct behaviour from the Fickian diffusion for the control gels, Table 2). Therefore, the rate determining step might become the weathering process, which occurred significantly slower than the diffusion of drug molecules in the gels explaining the high and low values of the *n* and *k* parameters, respectively.

Due to the various determining factors, the interpretation of the observed different drug-release capabilities of composites is extremely complicated, but the particle size analysis of the hydrogels and the specific surface area values of the organo-LDH composites (Table 1) allowed to draw some conclusions. For both anions, the drug liberation was highly favoured from the LDH solids prepared by the direct anion-exchange method, their size distribution histograms were similar and specific surface areas were the highest. For the co-precipitation and mechanochemically-aided intercalations, the measured surface area values of the hydrocalumites were largely analogous; however, the size distribution patterns clearly shifted toward the large particles in the diclofenac−LDH containing gels. Sum up, presumably, the smaller accessible surface of the solid particles could favour to the prolonged liberation of the drug molecules through decelerating the dissolution of Ca − OH moieties and the surface adsorbed organic molecules.

Finally, the *ex vivo* penetration of diclofenac and naproxen anions into the human fat free skin were followed by semi-quantitative Raman spectral mapping visualizing the spatial location of organic molecules in view of their intensities−amounts. For both drugs, the correlation maps from the non-treated, treated by control and LDH − hydrogel (encapsulated by the mechanochemically-aided technique) were compared after 24 h contact tests (Fig. 8). The diclofenac and naproxen molecules could easily penetrate into the epidermis and dermis from the control hydrogel, and the region of the *stratum corneum* was just slightly enriched by the drug molecules. However, their LDH capsulated forms showed more limited movements, the main part of organic moieties (naproxen not shown) could be registered only in the epidermis and the upper papillary zone of the dermis. The presence of hair follicles significantly modified the penetration of drugs (diclofenac not shown), the naproxen released even from LDH samples could reach the lower region of the dermis in higher amount (E labelled images). Considering that after 18 h, more than 90% of naproxen and diclofenac molecules could liberate from the interlamellar environment reaching the nearly same conditions as in the control gels, in the upper regions their accumulation could not be explained by the observed controlled release only. The adsorption of drug molecules on the external surfaces of metal hydroxide residues and their enrichment in the surrounding solution layers could also occur, in the meantime, the follicles gave ways for the solid particles toward the deeper levels of the skin.

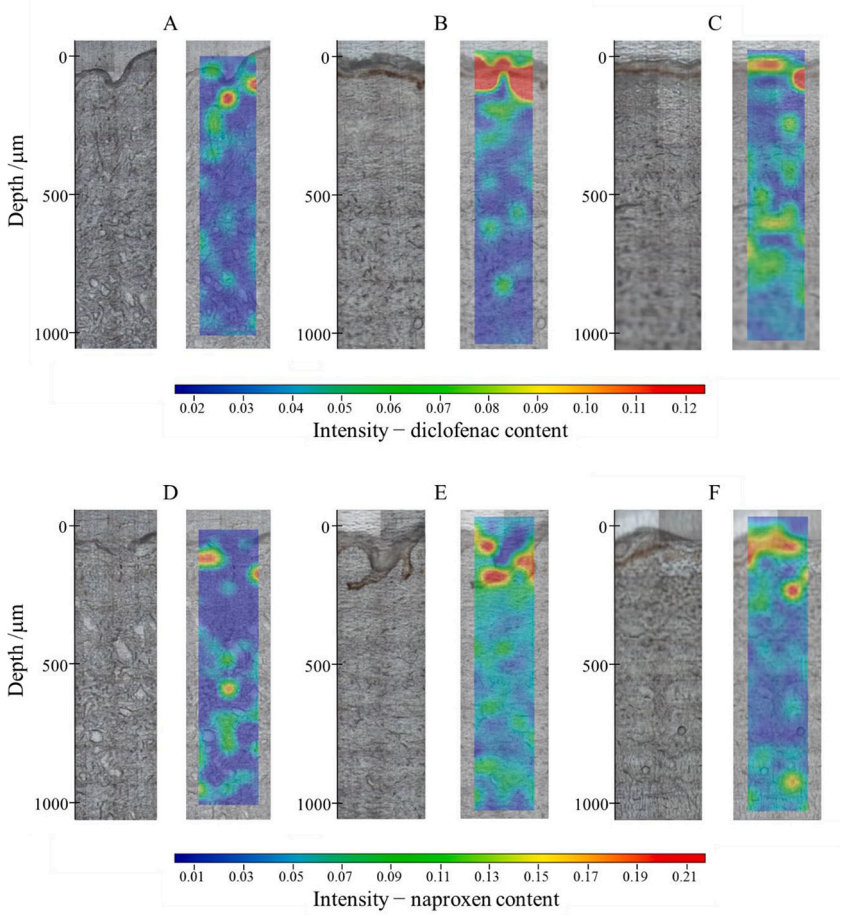

Fig. 8. Raman correlation maps for the distribution of diclofenac (B: LDH − hydrogel, C: control hydrogel) and naproxen (E: LDH − hydrogel, F: control hydrogel) anions in human skin layers compared to the non-treated specimens (A, D).

4. Conclusions

The anionic forms of diclofenac and naproxen anti-inflammatory drugs were successfully built into the interlamellar space of CaFe-layered double hydroxides. Four intercalation techniques; the co-precipitation, direct anion exchange, dehydroxylation-rehydration and mechanochemical treatment were tested and compared. For both anions, the dehydroxylation-rehydration method proved to be the most suitable to synthesise the drug−LDH composites with the largest organic content. The infrared and Raman spectroscopy measurements verified the presence of the diclofenac and naproxen anions among the layers and on the external surface. The thermogravimetric analysis showed intact LDH composites until 200 °C and enhanced thermal stability for the intercalated diclofenac and decreased one for the naproxen anions. The dynamic light scattering and zeta potential measurements showed heavily aggregated and negatively charged clays.

The particle size distribution of the diclofenac−LDH dispersed in the hydrogels highly depended on the applied intercalation techniques, however, the work with naproxen attested less sensibility. The *in vitro* drug diffusion tests verified the potential of CaFe-LDH solids regarding the storing and controlled release of intercalated diclofenac and naproxen molecules. The kinetic study showed drug liberation driven by the weathering of hydrocalumite particles in contrast to the mainly ion exchange control for the magnesium or zinc hydroxide based variants in environment with neutral or higher pH. For both anions, the LDH samples prepared by the conventional co-precipitation and the novel mechanochemically-aided encapsulation techniques possessed with the largest anion retention capability. The *ex vivo* penetration Raman maps indicated the accumulation of drug molecules released from the LDH particles in the upper region of the skin, but showed the deeper intrude of anions through hair follicles.

To sum up, the mechanochemically-aided intercalation techniques attested intensified relevance in the fabrication of organic LDH solids due to its multi-step and hence more specific and easier to shape synthesis character compared to the limits of the single step co-precipitation method. Moreover the prepared completely biocompatible composites could have great potential in carrying, protecting and dosing of dermal anti-inflammatory drugs, especially for topical anesthetic applications in area of sore follicles or heavily horny skin even utilizing the higher alkalinity of CaFe-LDH particles in the modifications of the permeability and hydration state of the skin.

Declaration of Competing Interest

The authors have no conflicting interests of any kind. They all agreed in submitting the manuscript to *Applied Clay Science*.

Acknowledgement

This work was supported by the European Union and the Hungarian Government through grant GINOP-2.3.2-15- 2016-00013 and the NTP-NTFÖ-19-B-0001. The financial help is highly appreciated.

Appendix A. Supplementary data

Supplementary data to this article can be found online at https://doi.org/10.1016/j.clay.2021.106233.

References

Abdellaoui, K., Pavlovic, I., Barriga, C., 2019. Nanohybrid layered double hydroxides used to remove several dyes from water. ChemEngineering 3, 41. https://doi.org/10.3390/chemengineering3020041.

Al-Jaberi, M., Naille, S., Dossot, M., Ruby, C., 2015. Interlayer interaction in Ca–Fe layered double hydroxides intercalated with nitrate and chloride species. J. Mol. Struct. 1102, 253–260. https://doi.org/10.1016/j.molstruc.2015.08.064.

Ambrogi, V., Fardella, G., Grandolini, G., Perioli, L., 2001. Intercalation compounds of hydrotalcite-like anionic clays with antiinflammatory agents — I. Intercalation and in vitro release of ibuprofen. Int. J. Pharm. 220, 23–32. https://doi.org/10.1016/S0378-5173(01)00629-9.

Bastianini, M., Faffa, C., Sisani, M., Petracci, A., 2018. Caffeic acid-layered double hydroxide hybrid: a new raw material for cosmetic applications. Cosmetics 5, 51. https://doi.org/10.3390/cosmetics5030051.

Bi, X., Zhang, H., Dou, L., 2014. Layered double hydroxide-based nanocarriers for drug delivery. Pharmaceutics 6, 298–332. https://doi.org/10.3390/pharmaceutics6020298.

Bruschi, M.L., 2015. Mathematical models of drug release. In: Strategies to Modify the Drug Release from Pharmaceutical Systems. Woodhead Publishing, pp. 63–68. https://doi.org/10.1016/B978-0-08-100092-2.00005-9.

Bugris, V., Haspel, H., Kukovecz, Á., Kónya, Z., Sipiczki, M., Sipos, P., Pálinko, I., 2013. Water types and their relaxation behaviour in partially rehydrated CaFe-Mixed binary oxide obtained from CaFe-layered double hydroxide in the 155–298 K temperature range. Langmuir 29, 13315–13321. https://doi.org/10.1021/la4035276.

Chakraborty, S., Kumar, M., Suresh, K., Pugazhenthi, G., 2014. Influence of organically modified NiAl layered double hydroxide (LDH) loading on the rheological properties of poly (methyl methacrylate) (PMMA)/LDH blend solution. Powder Technol. 256, 196–203. https://doi.org/10.1016/j.powtec.2014.02.035.

Chatterjee, A., Bharadiy, P., Hansora, D., 2019. Layered double hydroxide based bionanocomposites. Appl. Clay Sci. 177, 19–36. https://doi.org/10.1016/j.clay.2019.04.022.

Chen, Y., Shui, Z., Chen, W., Chen, G., 2015. Chloride binding of synthetic Ca–Al–NO_3 LDHs in hardened cement paste. Constr. Build. Mater. 93, 1051–1058. https://doi.org/10.1016/j.conbuildmat.2015.05.047.

Chibwe, K., Jones, W., 1989. Intercalation of organic and inorganic anions into layered double hydroxides. J. Chem. Soc. Chem. Commun. 14, 926–927. https://doi.org/10.1039/C39890000926.

Choy, J.-H., Kwak, S.-Y., Park, J.-S., Jeong, Y.-J., Portier, J., 1999. Intercalative nanohybrids of nucleoside monophosphates and DNA in layered metal hydroxide. J. Am. Chem. Soc. 121, 1399–1400. https://doi.org/10.1021/ja981823f.

Choy, J.-H., Jung, J.-S., Oh, J.-M., Park, M., Jeong, J., Kang, Y.-K., Han, O.-J., 2004. Layered double hydroxide as an efficient drug reservoir for folate derivatives. Biomaterials 25, 3059–3064. https://doi.org/10.1016/j.biomaterials.2003.09.083.

Choy, J.-H., Choi, S.-J., Oh, J.-M., Park, T., 2017. Clay minerals and layered double hydroxides for novel biological applications. Appl. Clay Sci. 36, 122–132. https://doi.org/10.1016/j.clay.2006.07.007.

Costa, P., Lobo, J.M.S., 2001. Modeling and comparison of dissolution profiles. Eur. J. Pharm. Sci. 13, 123–133. https://doi.org/10.1016/S0928-0987(01)00095-1.

Cursino, A.C.T., da Silva Lisboa, F., dos Santos Pyrrho, A., de Sousa, V.P., Wypych, F., 2013. Layered double hydroxides intercalated with anionic surfactants/benzophenone as potential materials for sunscreens. J. Colloid. Interf. Sci. 397, 88–95. https://doi.org/10.1016/j.jcis.2013.01.059.

Dékány, I., Haraszti, T., 1997. Layered solid particles as self-assembled films. Colloid. Surface. A 391–401. https://doi.org/10.1016/S0927-7757(96)03804-6.

Del Hoyo, C., 2007. Layered double hydroxides and human health: an overview. Appl. Clay Sci. 36, 103–121. https://doi.org/10.1016/j.clay.2006.06.010.

Ding, Y., Alpay, E., 2001. High temperature recovery of CO_2 from flue gases using hydrotalcite adsorbent. Process. Saf. Environ. Sci. 79, 45–51. https://doi.org/10.1205/095758201531130.

Duan, X., Lu, J., Evans, D.G., 2011. Assembly chemistry of anion-intercalated layered materials. Mod. Inorg. Synth. Chem. 17, 375–404. https://doi.org/10.1016/B978-0-444-53599-3.10017-4.

Evans, G.D., Slade, R.C.T., 2006. Structural aspects of layered double hydroxides. Struct. Bond. 119, 1–87. https://doi.org/10.1007/430_005.

Fan, G., Li, F., Evans, G.D., Duan, X., 2014. Catalytic applications of layered double hydroxides: recent advances and perspectives. Chem. Soc. Rev. 43, 7040–7066. https://doi.org/10.1039/c4cs00160e.

Ferencz, Z., Szabados, M., Ádok-Sipiczki, M., Kukovecz, Á., Kónya, Z., Sipos, P., Pálinkó, I., 2014. Mechanochemically assisted synthesis of pristine Ca(II)Sn(IV)-layered double hydroxides and their amino acid intercalated nanocomposites. J. Mater. Sci. 49, 8478–8486. https://doi.org/10.1007/s10853-014-8558-8.

Fini, A., Cavallari, C., Ospitali, F., 2010. Diclofenac salts. v. Examples of polymorphism among diclofenac salts with alkyl-hydroxy amines studied by DSC and HSM. Pharmaceutics 2, 136–158. https://doi.org/10.3390/pharmaceutics2020136.

Fontes, D.A.F., de Lyra, M.A.M., de Andrade, J.K.F., de Medeiros Schver, G.C.R., Rolim, L.A., da Silva, T.G., Soares-Sobrinho, J.L., Alves-Júnior, S., Rolim-Neto, P.J., 2016. CaAl-layered double hydroxide as a drug delivery system: effects on solubility and toxicity of the antiretroviral efavirenz. J. Incl. Phenom. Macrocycl. Chem. 85, 281–288. https://doi.org/10.1007/s10847-016-0627-y.

Forano, C., Hibino, T., Leroux, F., Taviot-Guého, C., 2006. Layered double hydroxides. Developments in Clay Science 1, 1021–1095. https://doi.org/10.1016/S1572-4352(05)01039-1.

Gastuche, M.C., Brown, G., Mortland, M.M., 1967. Mixed magnesium-aluminium hydroxides. I. Preparation and characterization of compounds formed in dialysed systems. Clay Miner. 7, 177–192. https://doi.org/10.1180/claymin.1967.007.2.05.

He, X., Qiu, X., Hu, C., Liu, Y., 2018. Treatment of heavy metal ions in wastewater using layered double hydroxides: a review. J. Disper. Sci. Technol. 39, 792–801. https://doi.org/10.1080/01932691.2017.1392318.

Hochstetter, C., 1842. Untersuchung über die Zusammensetzung einiger Mineralien. J. Prakt. Chem. 27, 375–378. https://doi.org/10.1002/prac.18420270156.

Hoxha, A., Gillam, D.G., Bushby, A.J., Agha, A., Patel, M.P., 2019. Layered double hydroxide fluoride release in dental applications: a systematic review. Dent. J. 7, 87–101. https://doi.org/10.3390/dj7030087.

Jaberi, M.A., Mallet, M., Greenwell, H.C., Abdelmoula, M., Ruby, C., 2019. Using Ca–Fe layered double hydroxide transformation to optimise phosphate removal from waste waters. Appl. Clay Sci. 182, 105281. https://doi.org/10.1016/j.clay.2019.105281.

Jamrógiewicz, M., Milewska, K., Mikolaszek, B., 2021. Spectroscopic evaluation on pseudopolymorphs of sodium naproxen. Spectrochim. Acta A 261, 120018. https://doi.org/10.1016/j.saa.2021.120018.

Kameda, T., Tochinai, M., Kumagai, S., Yoshioka, T., 2020. Treatment of HCl gas by cyclic use of Mg–Al layered double hydroxide intercalated with CO_3^{2-}. Atmos. Pollut. Res. 11, 290–295. https://doi.org/10.1016/j.apr.2019.11.001.

Khan, A.I., Lei, L., Norquist, A.J., O'Hare, D., 2001. Intercalation and controlled release of pharmaceutically active compounds from layered double hydroxide. Chem. Commun. 2342–2343. https://doi.org/10.1039/B106465G.

Khan, S.B., Alamry, K.A., Alyahyawi, N.A., Asiri, A.M., 2008. Controlled release of organic–inorganic nanohybrid:cefadroxil intercalated Zn–Al-layered double hydroxide. Int. J. Nanomedicine 13, 3203–3222. https://doi.org/10.2147/IJN.S138840.

Kim, T.-H., Oh, J.-M., 2016. Dual nutraceutical nanohybrids of folic acid and calcium containing layered double hydroxides. J. Solid State Chem. 233, 125–132. https://doi.org/10.1016/j.jssc.2015.10.019.

Kong, X., Jin, L., Wei, M., Duan, X., 2010. Antioxidant drugs intercalated into layered double hydroxide: Structure and in vitro release. Appl. Clay Sci. 49, 324–329. https://doi.org/10.1016/j.clay.2010.06.017.

Kuwahara, Y., Tsuji, K., Ohmichi, T., Kamegawa, T., Mori, K., Yamashita, H., 2012. Waste-slag hydrocalumite and derivatives as heterogeneous base catalysts. ChemSusChem 5, 1523–1532. https://doi.org/10.1002/cssc.201100814.

Kuzmann, E., Garg, V.K., de Oliveira, A.C., Herojit Singh, L., Pati, S.S., Guimaraes, E.M., dos Santos, T.O., Ádok-Sipiczki, M., Sipos, P., Pálinkó, I., 2015. Mössbauer, XRD and TEM study on the intercalation and the release of drugs in/from layered double hydroxides. Croat. Chem. Acta 88, 369–376. https://doi.org/10.5562/cca2683.

Li, F., Jin, L., Han, J., Wei, M., Li, C., 2009. Synthesis and controlled release properties of prednisone intercalated Mg-Al layered double hydroxide composite. Ind. Eng. Chem. Res. 48, 5590–5597. https://doi.org/10.1021/ie900043r.

Linares, C.F., Moscosso, J., Alzurutt, V., 2016. Carbonated hydrocalumite synthesized by the microwave method as a possible antacid. Mat. Sci. Eng. C-Mater. 61, 875–878. https://doi.org/10.1016/j.msec.2016.01.007.

Mills, S.J., Christy, J.-M., Génin, R., Kameda, T., Colombo, F., 2012. Nomenclature of the hydrotalcite supergroup: natural layered double hydroxides. Mineral. Mag. 76, 1289–1336. https://doi.org/10.1180/minmag.2012.076.5.10.

Miyata, S., 1983. Anion-exchange properties of hydrotalcite-like compounds. Clay Clay Miner. 31, 305–311. https://doi.org/10.1346/CCMN.1983.0310409.

Mora, M., López, M.I., Jiménez-Sanchidrián, C., Ruiz, J.R., 2011. Near- and mid-infrared spectroscopy study of synthetic hydrocalumites. Solid State Sci. 13, 101–105. https://doi.org/10.1016/j.solidstatesciences.2010.10.017.

Mosangi, D., Moyo, L., Pillai, S.K., Ray, S.S., 2016. Acetyl salicylic acid–ZnAl layered double hydroxide functional nanohybrid for skin care application. RSC Adv. 6, 105862–105870. https://doi.org/10.1039/C6RA22172F.

Muráth, S., Szabados, M., Sebők, D., Kukovecz, Á., Kónya, Z., Szilágyi, I., Sipos, P., Pálinkó, I., 2019. Influencing the texture and morphological properties of layered double hydroxides with the most diluted solvent mixtures – the effect of 6–8 carbon alcohols and temperature. Colloids Surf. A Physicochem. Eng. Asp. 574, 146–153. https://doi.org/10.1016/j.colsurfa.2019.04.053.

Olszówka, J.E., Karcz, R., Michalik-Zym, A., Napruszewska, B.D., Bielańska, E., Kryściak-Czerwenka, J., Socha, R.P., Nattich-Rak, M., Krzan, M., Klimek, A., Bahranowski, K., Serwicka, E.M., 2019. Effect of grinding on the physico-chemical properties of Mg-Al hydrotalcite and its performance as a catalyst for Baeyer-Villiger oxidation of cyclohexanone. Catal. Today 1, 147–153. https://doi.org/10.1016/j.cattod.2018.05.035.

Pagano, C., Perioli, L., Latterini, L., Nocchetti, M., Ceccarini, M.R., Marani, M., Ramella, D., Ricci, M., 2019. Folic acid-layered double hydroxides hybrids in skin formulations: Technological, photochemical and in vitro cytotoxicity on human keratinocytes and fibroblasts. Appl. Clay Sci. 168, 382–395. https://doi.org/10.1016/j.clay.2018.12.009.

Pérez-Barrado, E., Salagre, P., Marsal, L.F., Aguiló, M., Cesteros, Y., Díaz, F., Pallarès, J., Cucinotta, F., Marchese, L., Pujol, M.C., 2015. Ultrasound-assisted reconstruction and delamination studies on CaAl layered double hydroxides. Appl. Clay Sci. 118, 116–123. https://doi.org/10.1016/j.clay.2015.08.043.

Perioli, L., Ambrogi, V., Rossi, C., Latterini, L., Nocchetti, M., Costantino, U., 2006. Use of anionic clays for photoprotection and sunscreen photostability: Hydrotalcites and phenylbenzimidazole sulfonic acid. J. Phys. Chem. Solids 67, 1079–1083. https://doi.org/10.1016/j.jpcs.2006.01.029.

Perioli, L., Pagano, C., Nocchetti, M., Latterini, L., 2015. Development of smart semisolid formulations to enhance retinoic acid topical application. J. Pharm. Sci. 104, 3904–3912. https://doi.org/10.1002/jps.24612.

Qu, J., Sha, L., Wu, C., Zhang, Q., 2019a. Applications of mechanochemically prepared layered double hydroxides as adsorbents and catalysts: a mini-review. Nanomaterials 9, 80. https://doi.org/10.3390/nano9010080.

Qu, J., Sha, L., Xu, Z., He, Z., Wu, M., Wu, C., Zhang, Q., 2019b. Calcium chloride addition to overcome the barriers for synthesizing new Ca-Ti layered double hydroxide by mechanochemistry. Appl. Clay Sci. 173, 29–34. https://doi.org/10.1016/j.clay.2019.02.017.

Ray, S.S., Okamoto, M., 2003. Polymer/layered silicate nanocomposites: a review from preparation to processing. Prog. Polym. Sci. 28, 1539–1641. https://doi.org/10.1016/j.progpolymsci.2003.08.002.

Renaudin, G., Francois, M., Evrard, O., 1999. Order and disorder in the lamellar hydrated tetracalcium monocarboaluminate compound. Cem. Concr. Res. 29, 63–69. https://doi.org/10.1016/S0008-8846(98)00184-7.

Rojas, R., Jimenez-Kairuz, A.F., Manzo, R.H., Giacomelli, C.E., 2014. Release kinetics from LDH-drug hybrids: effect of layers stacking and drug solubility and polarity. Colloid. Surface. A 463, 37–43. https://doi.org/10.1016/j.colsurfa.2014.09.031.

Rousselot, I., Guého, C.T., Leroux, F., Léone, P., Palvadeau, P., Besse, J.-P., 2002. Insights on the structural chemistry of hydrocalumite and hydrotalcite-like materials: investigation of the series $Ca_2M^{3+}(OH)_6Cl{\cdot}2H_2O$ (M^{3+}: Al^{3+}, Ga^{3+}, Fe^{3+}, and Sc^{3+}) by X-ray powder diffraction. J. Solid State Chem. 167, 137–144. https://doi.org/10.1006/jssc.2002.9635.

Saha, S., Ray, S., Acharya, R., Chatterjee, T.K., Chakraborty, J., 2017. Magnesium, zinc and calcium aluminium layered double hydroxide-drug nanohybrids: a comprehensive study. Appl. Clay Sci. 135, 493–509. https://doi.org/10.1016/j.clay.2016.09.030.

Saji, R.S., Prasana, J.C., Muthu, S., George, J., Kuruvilla, T.K., Raajaraman, B.R., 2020. Spectroscopic and quantum computational study on naproxen sodium. Spectrochim. Acta A 226, 117614. https://doi.org/10.1016/j.saa.2019.117614.

Salguero, Y., Valenti, L., Rojas, R., García, M.C., 2020. Ciprofloxacin-intercalated layered double hydroxide-in-hybrid films as composite dressings for controlled antimicrobial topical delivery. Mater. Sci. Eng. C 111 (2020), 110859. https://doi.org/10.1016/j.msec.2020.110859.

Sharma, P., Chawla, A., Pawar, P., 2013. Design development, and optimization of polymeric based-colonic drug delivery system of naproxen. Sci. World J. 2013, 654829. https://doi.org/10.1155/2013/654829.

Siepmann, J., Peppas, N.A., 2001. Modeling of drug release from delivery systems based on hydroxypropyl methylcellulose (HPMC). Adv. Drug Deliver. Rev. 48, 139–157. https://doi.org/10.1016/S0169-409X(01)00112-0.

Sipos, P., Pálinkó, I., 2018. As-prepared and intercalated layered double hydroxides of the hydrocalumite type as efficient catalysts in various reactions. Catal. Today 306, 32–42. https://doi.org/10.1016/j.cattod.2016.12.004.

Sipos, P., May, P.M., Hefter, G.T., 2000. Carbonate removal from concentrated hydroxide solutions. Analyst 125, 955–958. https://doi.org/10.1039/a910335j.

Somosi, Z., Szabolcs, M., Nagy, P., Sebők, D., Szilágyi, I., Douglas, G., 2019. Contaminant removal by efficient separation of in situ formed layered double hydroxide compounds from mine wastewaters. Environ. Sci. Water Res. Technol. 5, 2251–2259. https://doi.org/10.1039/C9EW00808J.

Soussou, A., Gammoudi, I., Kalboussi, A., Grauby-Heywang, C., Cohen-Bouhacina, T., Baccar, Z.M., 2017. Hydrocalumite thin for polyphenol biosensor elaboration. IEEE Trans. Nanobiscience 16, 650–655. https://doi.org/10.1109/TNB.2017.2736781.

Szabados, M., Mészáros, R., Erdei, Sz, Kónya, Z., Kukovecz, Á., Sipos, P., Pálinkó, I., 2016. Ultrasonically-enhanced mechanochemical synthesis of CaAl-layered double hydroxides intercalated by a variety of inorganic anions. Ultrason. Sonochem. 31, 409–416. https://doi.org/10.1016/j.ultsonch.2016.01.026.

Szabados, M., Varga, G., Kónya, Z., Kukovecz, Á., Stefan, C., Sipos, P., Pálinkó, I., 2018. Ultrasonically-enhanced preparation, characterization of CaFe-layered double hydroxides with various interlayer halide, azide and oxo anions (CO_3^{2-}, NO_3^-, ClO_4^-). Ultrason. Sonochem. 40, 853–860. https://doi.org/10.1016/j.ultsonch.2017.08.041.

Szabados, M., Ádám, A.A., Kónya, Z., Kukovecz, Á., Carlson, S., Sipos, P., Pálinkó, I., 2019a. Effects of ultrasonic irradiation on the synthesis, crystallization, thermal and dissolution behaviour of chloride-intercalated, co-precipitated CaFe-layered double hydroxide. Ultrason. Sonochem. 55, 165–173. https://doi.org/10.1016/j.ultsonch.2019.02.024.

Szabados, M., Kónya, Z., Kukovecz, Á., Sipos, P., Pálinkó, I., 2019b. Structural reconstruction of mechanochemically disordered CaFe-layered double hydroxide. Appl. Clay Sci. 174, 138–145. https://doi.org/10.1016/j.clay.2019.03.033.

Taylor, H.F.W., 1973. Crystal structures of some double hydroxide minerals. Mineral. Mag. 39, 377–389. https://doi.org/10.1180/minmag.1973.039.304.01.

Tyner, K.M., Schiffman, S.R., Giannelis, E.P., 2004. Nanobiohybrids as delivery vehicles for camptothecin. J. Control. Release 95, 501–514. https://doi.org/10.1016/j.jconrel.2003.12.027.

Vieille, L., Taviot-Guého, C., Besse, J.-P., Leroux, F., 2003. Hydrocalumite and its polymer derivatives. 2. Polymer incorporation versus in situ polymerization of styrene-4-sulfonate. Chem. Mater. 15, 4369–4376. https://doi.org/10.1021/cm031070i.

Wang, Q., O'Hare, D., 2012. Recent advances in the synthesis and application of layered double hydroxide (LDH) nanosheets. Chem. Rev. 112, 4124–4155. https://doi.org/10.1021/cr200434v.

Wang, Y., Luo, S., Wang, Z., Fu, Y., 2013. Structural and textural evolution of nanocrystalline Mg–Al layered double hydroxides during mechanical treatment. Appl. Clay Sci. 80–81, 334–339. https://doi.org/10.1016/j.clay.2013.05.015.

Xu, Z.P., Jin, Y., Liu, S., Hao, Z.P., Lu, G.Q., 2008. Surface charging of layered double hydroxides during dynamic interactions of anions at the interfaces. J. Colloid Interf. Sci. 326, 522–529. https://doi.org/10.1016/j.jcis.2008.06.062.

Xu, Y., Hou, H., Liu, Q., Liu, J., Dou, L., Qian, G., 2015. Removal behavior research of orthophosphate by CaFe-layered double hydroxides. Desalin. Water Treat. 57, 1–8. https://doi.org/10.1080/19443994.2015.1039602.

Yan, L., Raphael, A.P., Zhu, X., Wang, B., Chen, W., Tang, T., Deng, Y., Sant, H.J., Zhu, G., Choy, K.W., Gale, B.K., Prow, T.W., Chen, X., 2014. Nanocomposite-strengthened dissolving microneedles for improved transdermal delivery to human skin. Adv. Healthc. Mater. 3, 555–564. https://doi.org/10.1002/adhm.201300312.

Yang, J.H., Lee, S.Y., Han, Y.S., Park, K.C., Choy, J.H., 2003. Efficient transdermal penetration and improved stability of L-ascorbic acid encapsulated in an inorganic nanocapsule. B. Korean Chem. Soc. 24, 499–503. https://doi.org/10.5012/bkcs.2003.24.4.499.

Zhang, M., Reardon, E.J., 2005. Chromate and selenate hydrocalumite solid solutions and their applications in waste treatment. Sci China C Life Sci 48, 165–173. https://doi.org/10.1007/bf02889815.

Zhou, Y., Sun, X., Zhong, K., Evans, D.G., Lin, Y., Duan, X., 2012. Control of surface defects and agglomeration mechanism of layered double hydroxide nanoparticles. Ind. Eng. Chem. Res. 51, 4215–4221. https://doi.org/10.1021/ie202302n.

Zhou, J., Li, X., Li, W., Wei, F., Su, Y., Zhang, J., Xu, Z.P., Qian, G., 2015. Multi-step removal mechanism of pyrophosphate using CaFe-layered double hydroxide at high pH. Appl. Clay Sci. 105–106, 21–26. https://doi.org/10.1016/j.clay.2014.12.001.